

Energy harvesting using a modified rectangular cymbal transducer based on $0.71\text{Pb}(\text{Mg}_{1/3}\text{Nb}_{2/3})\text{O}_3-0.29\text{PbTiO}_3$ single crystal

Bo Ren,^{1,2,3,a)} Siu Wing Or,^{2,b)} Xiangyong Zhao,¹ and Haosu Luo¹

¹Shanghai Institute of Ceramics, Chinese Academy of Sciences, Shanghai 201800, China

²Department of Electrical Engineering, The Hong Kong Polytechnic University, Hung Hom, Kowloon, Hong Kong

³Graduate School of the Chinese Academy of Sciences, Beijing 100049, China

(Received 21 October 2009; accepted 21 December 2009; published online 1 February 2010)

In this paper, we presented a modified rectangular cymbal transducer used as the vibration energy harvesting device based on $0.71\text{Pb}(\text{Mg}_{1/3}\text{Nb}_{2/3})\text{O}_3-0.29\text{PbTiO}_3$ single crystal. The vibration modes of the device were analyzed and the electrical properties were studied systematically. Under a cyclic force of 0.55 N (peak value), a high peak voltage of 45.7 V and maximum power of 14 mW were measured at 500 Hz with a proof mass of 17.0 g. The power density of the transducer is more than three times as high as that of the $\text{Pb}(\text{Zr}_x\text{Ti}_{1-x})\text{O}_3$ (PZT) ceramic cymbal transducer. The results demonstrate the potential of the device in energy harvesting applied to low-power portable electronics and wireless sensors. © 2010 American Institute of Physics. [doi:10.1063/1.3296156]

I. INTRODUCTION

During the past decade, energy harvesting from mechanical vibrations of ambient environments has been a hot research topic due to its potential application in many fields. Here, piezoelectric energy harvesting devices have attracted considerable attentions^{1–5} for the outstanding advantages of simpler structure compared to other methods such as using electromagnetic and electrostatic effects when scavenging power directly from the mechanical vibration.⁶ In 2004, a study at Pennsylvania State University reported a piezoelectric cymbal transducer for energy harvesting. At 100 Hz, the output power can reach 39 mW when connected with a load of 400 kΩ under an ac force of 7.8 N.⁷ Subsequently, another piezoelectric vibration energy scavenging generator using compressive axial preload was researched in 2006. The device can create 0.3–0.4 mW power output when subjected to a 7.1 g proof mass across a range of frequencies from 200–250 Hz. With the axial preload increased to 12.2 g, the power output simultaneously increased to 0.36–0.65 mW with the working frequencies from 160 to 195 Hz.⁸ The recent progress in energy harvesting from mechanical vibration was performed at University of Pittsburgh. These studies were made on a cantilever mounted $(1-x)\text{Pb}(\text{Mg}_{1/3}\text{Nb}_{2/3})\text{O}_3-x\text{PbTiO}_3$ /aluminum beam with a steel mass of 1.25 g attached at the free end. A power of 0.586 mW was generated from the device under a sinusoidal acceleration with a virtual value of 2.28 m/s^2 at the resonance frequency of 174 Hz.⁹ In 2007, a drum transducer was studied as the energy harvesting device at the Hong Kong Polytechnic University. Under a prestress of 0.15 N (15 g mass load) and a cyclic stress of 0.7 N, a power of 11 mW was generated at the resonance frequency of the device (590 Hz) across an 18 kΩ resistor.¹⁰

Cymbal is a transducer in which a piezoelectric disk is

sandwiched between two metal caps. The actual piezoelectric coefficient of the cymbal is amplified by the structure of the cymbal. The presence of cavities in the cymbal allows the metal end-caps to serve as a mechanical transformer for transforming and amplifying a portion of the incident axial stress in the radial stresses of opposite sign.¹¹ Thus, the d_{33} and d_{31} contributions of the piezoelectrics combine to provide the effective d^{eff} value of the cymbal as

$$d^{\text{eff}} = d_{33} - Ad_{31},$$

where A is amplification factor. The minus sign is introduced due to the negative value of d_{31} . The amplification factor A can be very large in the range of 10–100 depending on the design of the caps. Thus a piezoelectric cymbal has a very high transduction rate and can produce a large displacement.⁷

In recent years, relaxor piezoelectric single crystals $(1-x)\text{Pb}(\text{Mg}_{1/3}\text{Nb}_{2/3})\text{O}_3-x\text{PbTiO}_3$ (PMN- x PT or PMN-PT) have attracted continuous attention due to the well-known ultrahigh electromechanical response.^{12,13} The piezoelectric strain constants d_{33} , d_{31} , and electromechanical coupling coefficients k_{33} and k_{31} could reach as high as 2500 pC/N and -2500 pC/N and 0.94 and 0.95, respectively. However, the piezoelectric effect of PMN-PT is anisotropic, depending significantly on the crystal cut type and the poling direction. How to choose the optimal crystallographic directions and compositions to further improve the device performance is expecting. In this work, we made a research on a modified

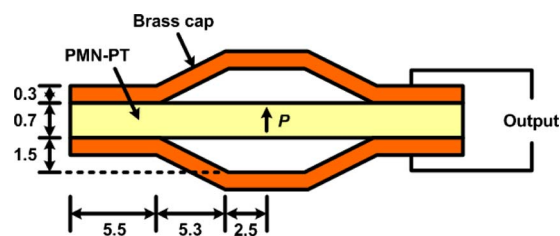


FIG. 1. (Color online) Schematic diagram of the cymbal transducer (Unit: mm). The polarization direction was denoted by the arrow P .

^{a)}Electronic mail: rbhoh@mail.sic.ac.cn.

^{b)}Electronic mail: eeswor@polyu.edu.hk.

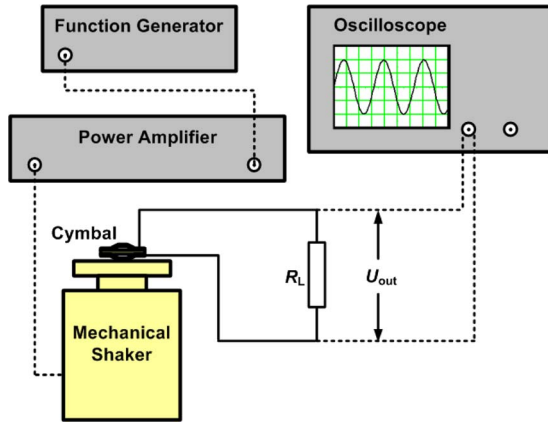
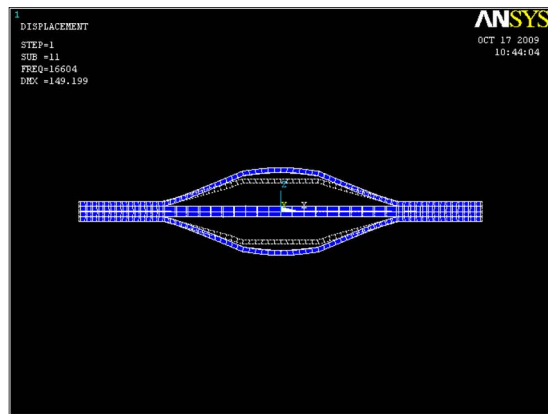
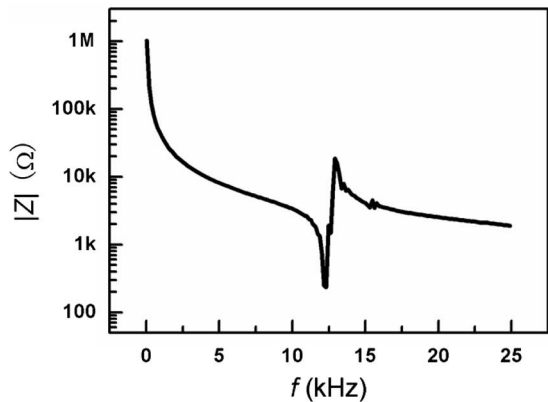


FIG. 2. (Color online) The experimental diagram for testing the electric properties.

cymbal transducer for harvesting mechanical energy based on the PMN-0.29PT single crystal. Compared to the disk cymbal, this modified cymbal transducer can make full use of the transverse extensional vibration of the PMN-PT crystal.¹⁴ Results indicate that under a cyclic force of 0.55 N (peak value), a high output peak voltage of 45.6 V, output power of 14 mW were obtained at the resonance frequency 500 Hz with a proof mass of 17.0 g when connecting a matching load resistance of 74 kΩ.

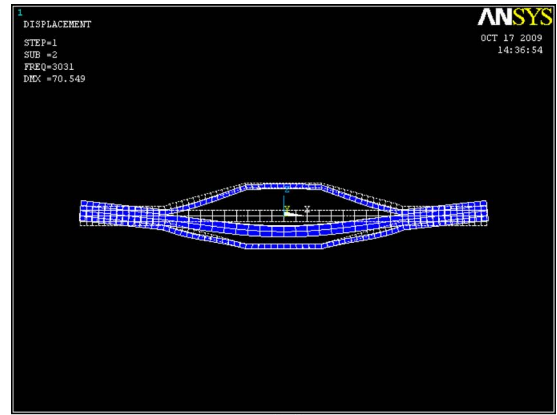


(a)

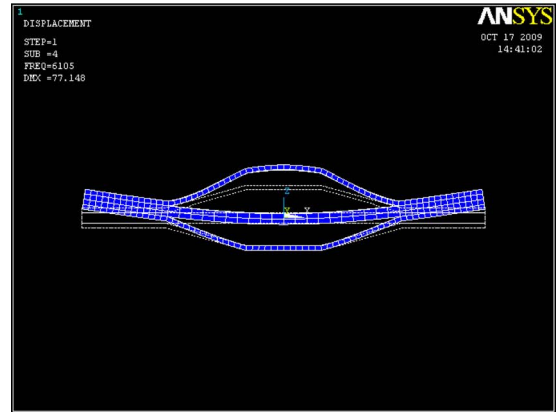


(b)

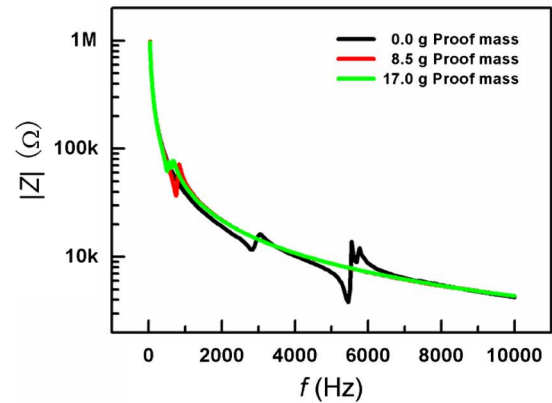
FIG. 3. (Color online) The vibration mode and impedance spectrum of the device measured under free condition.



(a)



(b)



(c)

FIG. 4. (Color online) The vibration modes and measured impedance spectrums of the device with different proof masses. One cap of the device was fixed on the shaker, and the other cap was bonded with the proof mass.

II. EXPERIMENTS

A. Structure and fabrication

In the experiment, the crystal was grown by a modified Bridgman technique^{13,15} and then cut into wafers. The orientations were oriented along the [001], [110], and [11̄0], respectively, corresponding to the length, width, and thickness directions, which is the optimal crystal cut for the transverse mode vibration.¹⁶

The proposed structure of the device is shown in Fig. 1. The PMN-PT wafer ($26.6 \times 4.0 \times 0.7 \text{ mm}^3$) was sandwiched between two brass caps and they were bonded together using a silver-loaded epoxy (Applied Products E-Solder 3021). The

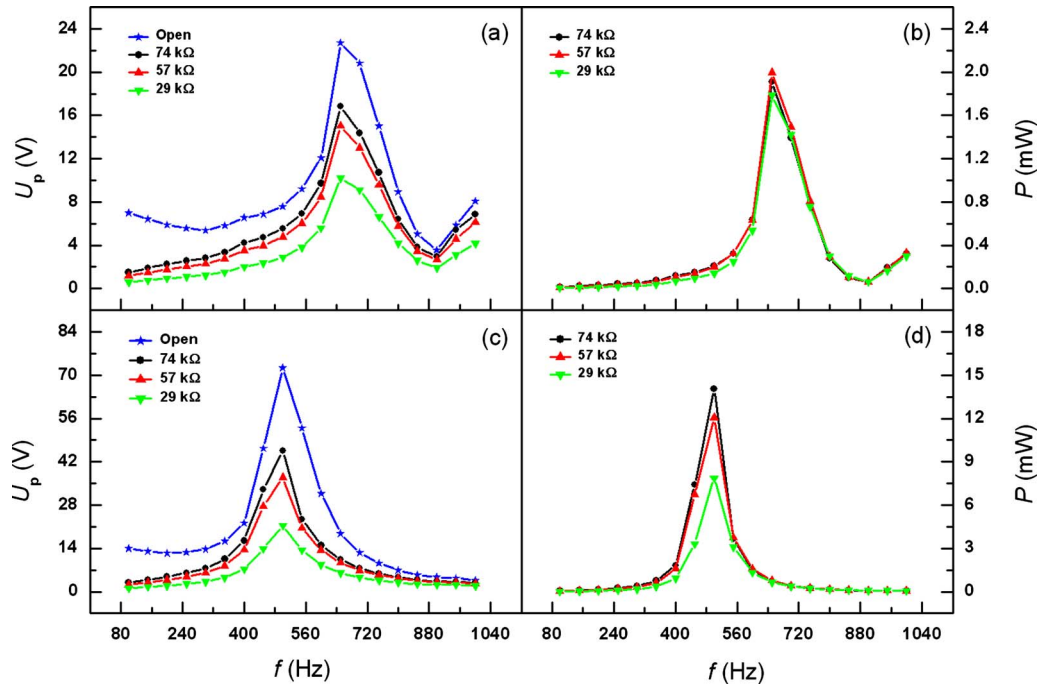


FIG. 5. (Color online) Frequency dependence of output peak voltage (U_p) and output power (P) under different load resistances with proof mass of 8.5 g [(a) and (b)] and 17.0 g [(c) and (d)].

PMN-PT wafer was poled along the thickness direction (indicated by the arrow) and the driving electrodes were painted on the two surfaces perpendicular to the thickness direction. In the experiment, one cap of the cymbal was bonded on the shaker as the base, and various proof masses were bonded on the other cap to change the mass load conditions. The gross mass of the device is 1.30 g.

B. Measurement setup and procedure

The experimental setup is presented as follows (Fig. 2). A mechanical shaker (Ling Dynamic Systems Ltd., model type V406), which can supply a maximum force of 89 N within a wide frequency range of 5–9000 Hz, was used to excite the vibration. One cap of the device was glued on the shaker with epoxy resin. The shaker was driven at various voltages and frequencies by using an arbitrary function generator (Sony Tektronix AFG 320) and power amplifier (Ling Dynamic Systems Ltd., model type PA 100E) to supply a sinusoidal force of the desired magnitude and frequency. The output voltage from the device was monitored by a Tektronix Digital Oscilloscope (Hewlett Packard 54645A). The whole experimental setup was put on a spongy cushion to avoid any interference from the surroundings. Various load resistances were used in order to characterize the performances of the device including the output voltage and power. The powers under different load resistances R_L were calculated using the formula $P = U_p^2 / 2R_L$, where U_p is the output peak voltage.

III. RESULTS AND DISCUSSION

Figure 3 shows the simulation results and measured impedance spectrum of the proposed cymbal transducer under free condition within a wide frequency range of 40 Hz–25 kHz. The simulation shown in Fig. 3(a) indicates the reso-

nance frequency of the device corresponding to the transverse mode of the wafer. No spurious vibration can be observed.

Subsequently, when fixing one cap of the cymbal on the shaker, simulation shown in Figs. 4(a) and 4(b) indicates that the above vibration mode disappears. This is ascribed to different boundary conditions of the device. At the moment, the measured impedance spectrums of the device with different proof masses are shown in Fig. 4(c). The curve without proof mass gives two resonance frequencies corresponding to the first two bending modes of the wafer illustrated in Figs. 4(a) and 4(b). When bonding different proof mass (8.5 and 17.0 g) on the other cap, the bending mode corresponding to Fig. 4(b) disappears. As a result, the impedance spectrum exhibits only one resonance frequency as shown in Fig. 4(c).

The frequency and load dependence of the output voltage and power of the proposed device were then measured with the experimental setup. Here two proof masses 8.5 and 17.0 g were used as the preloads and the peak values of the cyclic force on the device reach 0.29 and 0.55 N, respectively.

When bonded with an 8.5 g proof mass, the output voltage and power can reach the maximum at 650 Hz, which is corresponding to the resonance frequency shown in the impedance spectrum. The peak voltage output of 15.0 V and maximum output power of 2.0 mW were obtained with a matching load resistance of 57 k Ω . as shown in Figs. 5(a) and 5(b), and the corresponding power density is about 27 mW/cm³. When the load resistance is further increased, the voltage can become further larger while the power output decreases instead.

When the proof mass increased to 17.0 g, the resonance frequency of the device is shifted to lower frequency due to the mass increase of the global system. At the moment, the

peak voltage and power output can reach 45.7 V and 14 mW, respectively, as shown in Figs. 5(c) and 5(d). The corresponding power density is 188 mW/cm³, which is more than three times as high as that of the single-layer Pb(Zr_xTi_{1-x})O₃ (PZT) ceramic cymbal transducer (about 59 mW/cm³ under a cyclic force of 7.8 N),⁷ and about 25% higher than that of the cymbal transducer based on 10 layer PZT ceramic (about 151 mW/cm³ under a cyclic force of 70 N).¹⁷ The matching load resistance simultaneously increases to 74 kΩ. under the resonance frequency of 500 Hz. From the results it can be concluded that the maximum outputs increase with the proof mass, which can be ascribed to the increase of the excitation force.

IV. SUMMARY

In summary, a vibration energy harvesting device using a modified rectangular cymbal transducer based on 0.71Pb(Mg_{1/3}Nb_{2/3})O₃-0.29PbTiO₃ single crystal has been designed and fabricated. The electrical properties under different frequencies, load resistances, and proof masses were studied systematically. With the increasing of the proof mass, the resonance frequency of the system decreases and the output from the device increases. The device can make full use of the optimal orientation of the PMN-PT crystal and can yield a very large output. Under the cyclic force of 0.55 N (17.0 g proof mass), the device can generate a peak voltage of 45.7 V and a maximum power of 14 mW at 500 Hz with a matching load resistance of 74 kΩ. The power density of the transducer is more than three times as high as that of the PZT ceramic cymbal transducer. This proposed device has the potential to be applied to low-power portable electronics and wireless sensors.

ACKNOWLEDGMENTS

This work was financially supported by the Ministry of Science and Technology of China through 863 Program (No. 2008AA03Z410) and 973 Program (No. 2009CB623305),

the Natural Science Foundation of China (Nos. 60837003, 50777065, and 50602047), Shanghai Municipal Government (No. 08JC1420500), the Innovation Fund of Shanghai Institute of Ceramics (No. O99ZC4140G), the Fund of National Engineering Research Center for Optoelectronic Crystalline Materials (No. 2005DC105003-2007K05), Research Grants Council of the HKSAR Government (PolyU 5266/08E) and the Innovation and Technology Fund of the HKSAR Government (GHP/003/06).

¹J. Kyriassis, C. Kendall, J. Paradiso, and N. Gershenfeld, Second International Symposium on Wearable Computers—Digest of Papers, 1998 (unpublished), Vol. 174, pp. 132–139.

²G. K. Ottman, H. F. Hofmann, A. C. Bhatt, and G. A. Lesieutre, *IEEE Trans. Power Electron.* **17**, 669 (2002).

³R. A. Islam and S. Priya, *Appl. Phys. Lett.* **88**, 032903 (2006).

⁴K. L. Ren, Y. M. Liu, X. C. Geng, H. F. Hofmann, and Q. M. Zhang, *IEEE Trans. Ultrason. Ferroelectr. Freq. Control* **53**, 631 (2006).

⁵A. Erturk, O. Bilgen, and D. J. Inman, *Appl. Phys. Lett.* **93**, 224102 (2008).

⁶K. A. Cook-Chennault, N. Thambi, and A. M. Sastry, *Smart Mater. Struct.* **17**, 043001 (2008).

⁷H. W. Kim, A. Batra, S. Priya, K. Uchino, D. Markley, R. E. Newnham, and H. F. Hofmann, *Jpn. J. Appl. Phys., Part 1* **43**, 6178 (2004).

⁸E. S. Leland and P. K. Wright, *Smart Mater. Struct.* **15**, 1413 (2006).

⁹C. L. Sun, L. F. Qin, F. Li, and Q. M. Wang, *J. Intell. Mater. Syst. Struct.* **20**, 559 (2008).

¹⁰S. Wang, K. H. Lam, C. L. Sun, K. W. Kwok, H. L. W. Chan, M. S. Guo, and X. Z. Zhao, *Appl. Phys. Lett.* **90**, 113506 (2007).

¹¹R. B. Newnham, A. Dogan, D. C. Markley, J. F. Tressler, J. Zhang, E. Usgur, R. J. Meyer, Jr., A. C. Hladky-Hennion, and W. J. Ughses, *OCEANS'02 MTS/IEEE, 2002* (unpublished), Vol. 4, pp. 2315–2321.

¹²R. F. Service, *Science* **275**, 1878 (1997).

¹³H. S. Luo, G. S. Xu, P. C. Wang, and Z. W. Yin, *Ferroelectrics* **231**, 97 (1999).

¹⁴L. H. Luo, Y. X. Tang, F. F. Wang, C. J. He, and H. S. Luo, *Solid State Commun.* **143**, 321 (2007).

¹⁵H. S. Luo, G. S. Xu, P. C. Wang, H. Q. Xu, and Z. W. Yin, *Jpn. J. Appl. Phys., Part 1* **39**, 5581 (2000).

¹⁶J. Peng, H. S. Luo, D. Lin, H. Q. Xu, T. H. He, and W. Q. Jin, *Appl. Phys. Lett.* **85**, 6221 (2004).

¹⁷H. Kim, S. Priya, H. Stephanou, and K. Uchino, *IEEE Trans. Ultrason. Ferroelectr. Freq. Control* **54**, 1851 (2007).